Int. J. Heat Mass Transfer. Vol. 12, pp. 699–711. Pergamon Press 1969. Printed in Great Britain

THE VOID FRACTION IN AN ANNULAR CHANNEL AT ATMOSPHERIC PRESSURE

ROBERTO EVANGELISTI and PAOLO LUPOLI

Laboratorio Tecnologie Reattori, C.N.E.N., Centro Studi Nucleari della Casaccia, Rome, Italy

(*Received* 5 *June* 1968 *and in revised form* 31 *December* 1968)

Abstract—The application of the γ-absorption method to measurement of vapour volumetric fraction during forced convection boiling in a small annular channel is discussed.

The experimental results are presented and compared with existing theoretical models in the subcooled region.

NOMENCLATURE

W, test section power input [W];
Γ, mass velocity [g/s cm^2];
A_F, flow area [cm^2];
G, mass flow rate [g/s] = $\Gamma \cdot A_F$;
c_p, specific heat [cal/g °C];
H_{fg}, heat of vaporization [cal/g];
T, temperature [°C];
ΔT, temperature drop across the orifice;
x, thermodynamic local mass quality of two-phase mixture (calculated from a heat balance and thermal equilibrium);
α, void fraction;
θ, subcooling degree [°C];
L, heated channel length [cm];
L_γ, distance of the γ-beam axis from test section inlet [cm];
ϕ, heat flux [W/cm^2];
P, heated perimeter of channel [cm];
ρ, density;
R_d, bubble radius at detachment [cm];
K_{th}, thermal conductivity [W/cm° C];
h, single phase heat-transfer coefficient [W/cm^2 °C];
x^*, true local vapour weight fraction (or actual mass quality);
S, slip ratio;
Y_B^+, nondimensional distance from wall corresponding to tip of vapour bubble;
σ, surface tension [dyn/cm];
D_H, hydraulic diameter [cm];
μ, dynamic viscosity [g/cm s];
τ_w, wall shear stress [dyn/cm^2];
f, friction factor;
ε, channel roughness [cm];
g, gravitational constant [cm/s^2];
Pr, Prandtl number.

Subscripts

sat. at saturation temperature (pressure);
in, inlet;
ou, outlet;
γ, corresponding to the position of the γ-beam axis;
s, standard;
os, one-shot;
TT, traversing technique;
d, at the bubbles detachment;
w, wall;
b, bulk;
l, liquid;
va, vapour;
Bo, Bowring;
Le, Levy.

INTRODUCTION

THE ACCURATE determination of the volumetric

steam fraction α in water–steam mixtures is essential to the design of water-moderated boiling reactors and to a complete understanding of the fluid mechanics of two-phase flow. Many methods have been developed for measuring the void fraction of a flowing two-phase mixture: the most commonly used method employs the attenuation of low energy gamma radiation. During the past years the use of radioactive techniques for measurement of two-phase density has become more and more prevalent. The radiation attenuation method of density determination is based on the absorption of gamma rays, from a radioactive source, which can be measured and related to the void volume fraction. The technique is a powerful research tool when applied to fundamental two-phase flow studies, since the local density and the relative velocity of the two phases can be readily determined.

The purpose of this experiment was to study the formation and behaviour of vapour, and therefore the void fraction, in a vertical, annular channel (length 500 mm, o.d. 13 mm, i.d. 7 mm) under boiling-heat-flux conditions at atmospheric pressure. The experiments have been carried out for two values of flow rate and three different heat fluxes, whether in subcooled or in bulk boiling region. The particular test conditions were chosen to reproduce the conditions at which tests must be made with a sodium loop at Casaccia Laboratory.

1. EXPERIMENTAL APPARATUS AND PROBLEMS RELATED TO GAMMA ATTENUATION METHOD

For the experiment a small loop (CFP-5) built at C.S.N. Casaccia for the development of experimental techniques in the boiling heat-transfer field [1] was used. This loop is a closed circulating system comprising a pump, a turbo-flowmeter, a single-tube preheater (supplied by a 15 kW power controlled rectifier), a test section of annular cross-section (Fig. 1), a compact condenser, a cooler and an expansion reservoir with a calibrated cylindrical burette. The loop is shown schematically in Fig. 2.

The local value of steam quality corresponding to the position of the gamma-beam axis and the test section inlet steam quality are evaluated by means of thermocouples located across the orifice and in the upper mixing chamber. By measuring the electrical power heating in the internal tube of the test section, the temperatures and the mass flow rate it is possible to obtain the local value of the steam quality. Assuming a uniform heat generation along the test section, let W the total power input, W_1 the power used to heat liquid to T_s, W_2 the power used to vaporize saturated liquid and x_γ the local value of steam quality in the section corresponding to the position of the γ-beam axis. Heat balance yields:

$$W = W_1 + W_2$$

$$W_1 = Gc_p(T_{\text{sat.}} - T_{in})$$

$$W_2 = x_\gamma G H_{fg}$$

and therefore

$$x_\gamma = \frac{1}{H_{fg}}\left[\frac{W}{G} - c_p(T_{\text{sat.}} - T_{in})\right]. \tag{1}$$

The inlet steam quality is evaluated by means of the thermocouples located across the orifice: they indicate a temperature drop ΔT which is related to the test section inlet quality when there is no evaporation before orifice by the equation

$$x_{in} = \frac{c_p}{H_{fg}}\Delta T. \tag{2}$$

Such a condition obviously limits the maximum x_{in} value which can be obtained without boiling in the preheater. The constancy of the local value x_γ depends on the voltage control of the 30 kW rectifier which supplies the heating power to the annular test section: such a power can be always considered constant better than ± 1 per cent.

Flow rates were determined by a Faure–Hermann turboflowmeter, whose response was

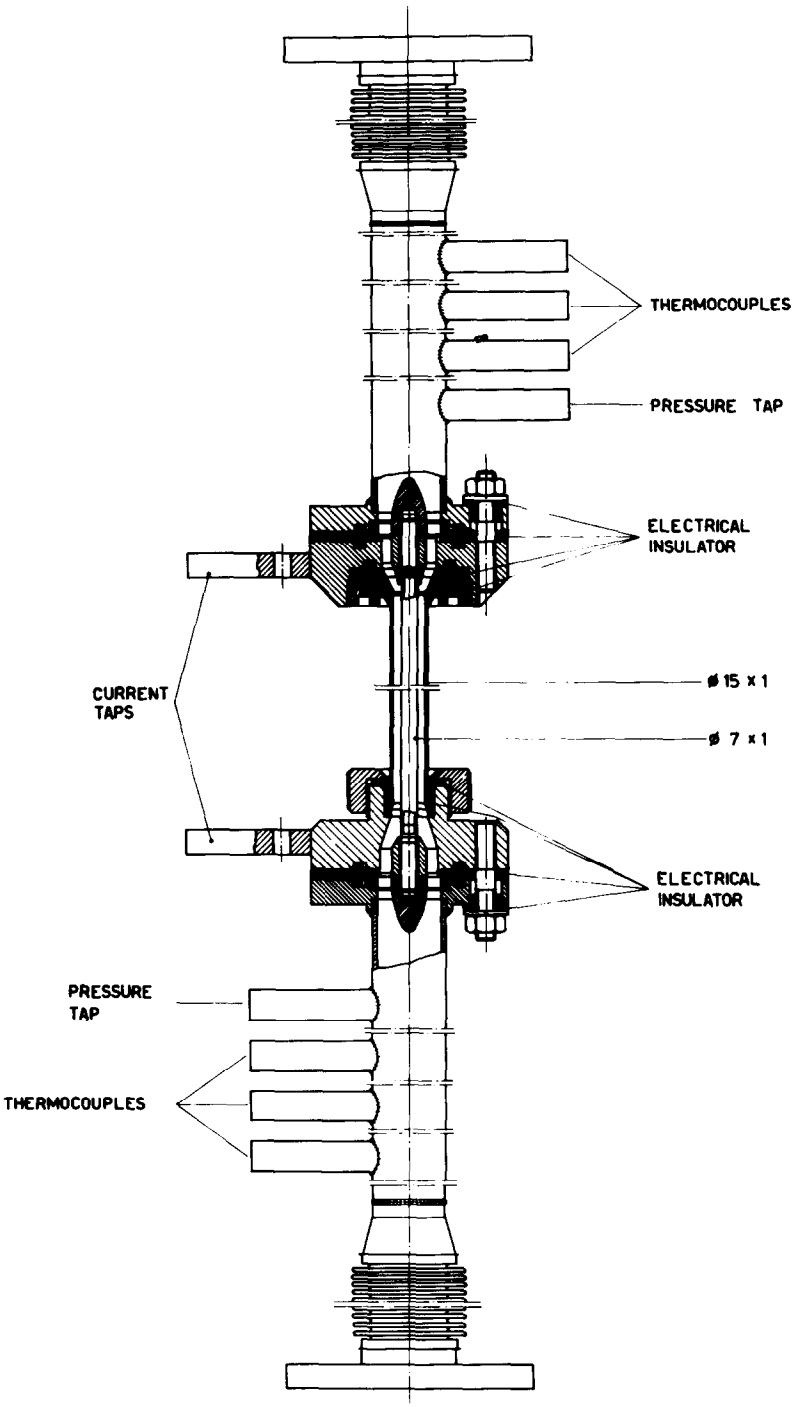

FIG. 1. Test section.

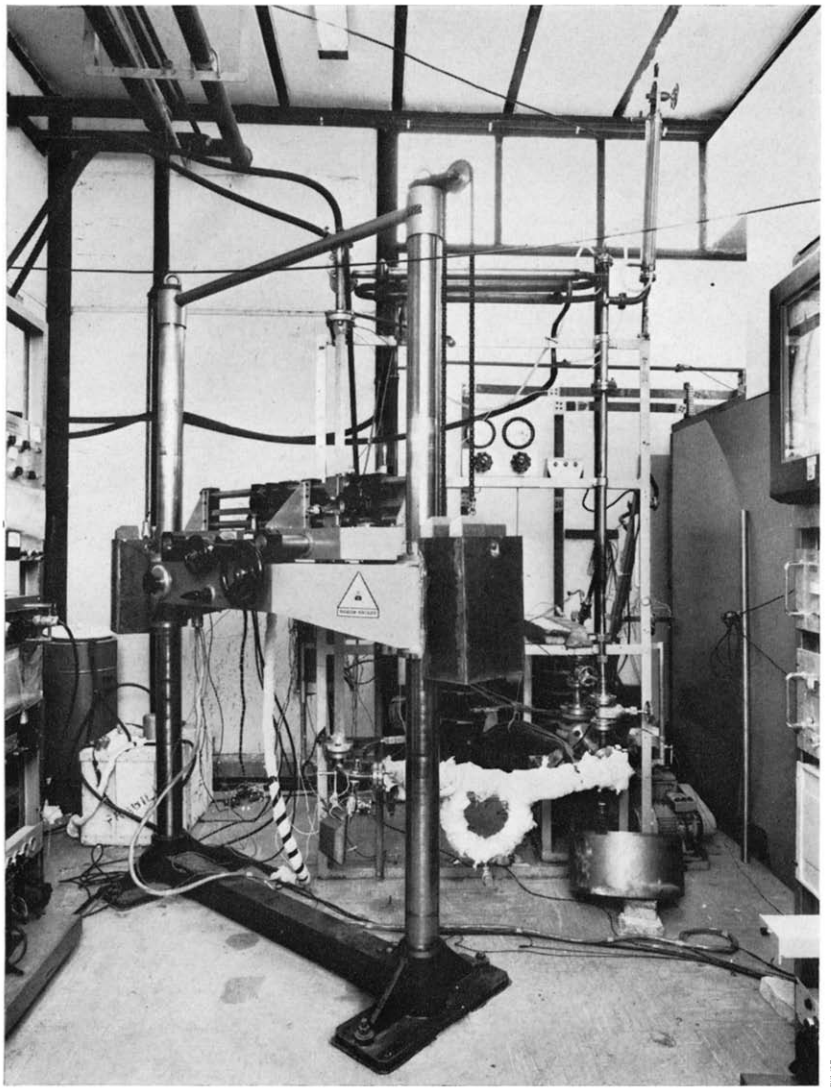

FIG. 4. Void fraction carriage assembly.

facing page 701

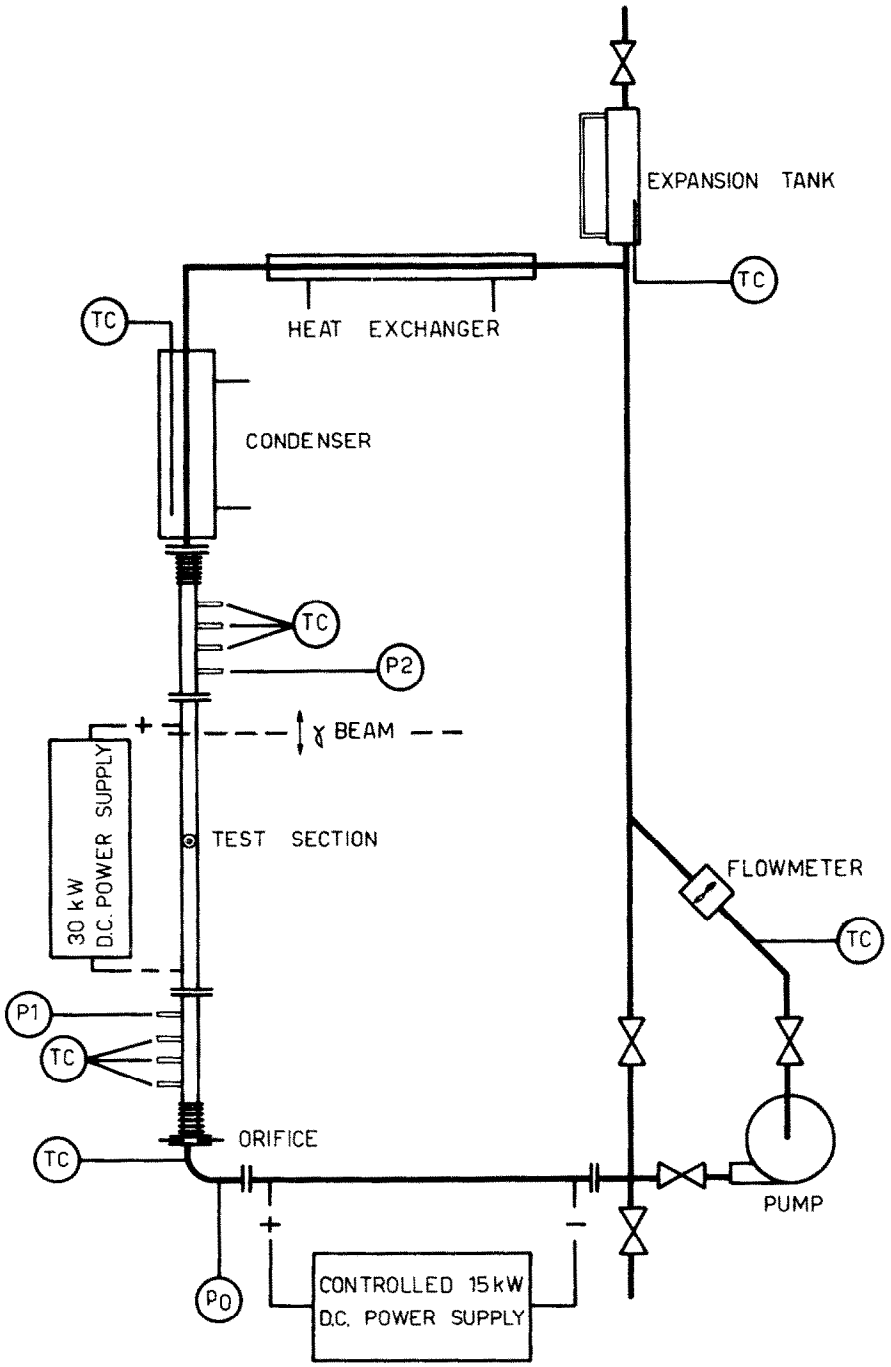

FIG. 2. Loop flow diagram.

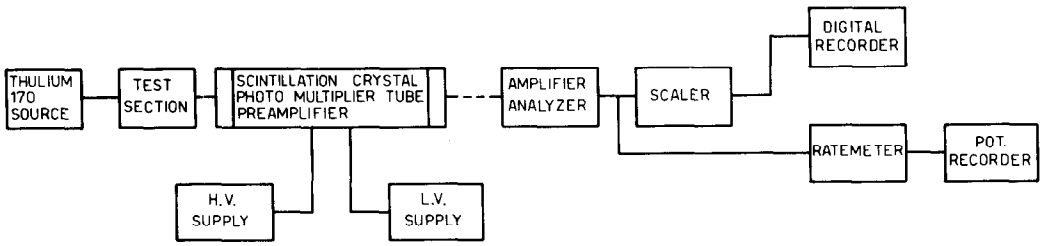

FIG. 3. Equipment void meter.

pre-calibrated with a precision better than $\pm 0{\cdot}5$ per cent. All flow rates measured checked favourably against values calculated on the basis of heat balances over the preheater.

Power delivered to the test section and preheater was calculated from measurements of the appropriate voltage drops across the tubes and shunts. All voltages shunts, thermocouples, etc., and frequencies (of the flowmeter) were measured by a Hewlett–Packard digital voltmeter-frequency-meter with a sensitivity of $\pm 1\ \mu V$.

The equipment used for measuring the density of the two phase mixture is shown in Fig. 3. The radioactive source was Thulium 170, with an original strength of 1 c, which has a half-life of approximately 129 days and two energy peaks, 0·053 MeV and 0·084 MeV. The γ-rays are collimated before entering the flow channel by a rectangular lead collimator whose width and height depend on the chosen measurement geometry. The source collimator and detector were mounted on a carriage (Fig. 4) which could move in either a horizontal or

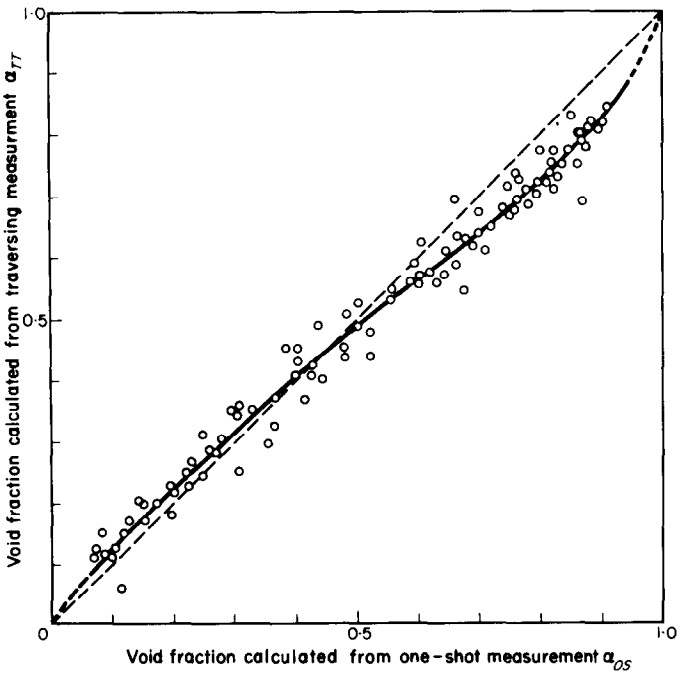

FIG. 5. Influence of voids distribution.

vertical direction. Besides they can be positioned along the axis of measurement in order to obtain the chosen collimation geometry.

A series of runs were made directly on the loop CFP-5 to obtain a comparison between the traversing and the one-shot method on two-phase fluid in the actual geometrical annular configuration and in the whole range of subcooled and bulk boiling (Fig. 5). The discrepancies between the two methods were greater at high voids where semiannular or churn flow existed and at low voids where bubble flow was present. The best fit of the results obtained from such a two-phase fluid study was assumed as a "calibration" curve for the experiment.

The best fit equation is, in the range $0{\cdot}070 \leqslant \alpha_{os} \leqslant 0{\cdot}930$.

$$\alpha_{TT} = 3{\cdot}47 \,.\, 10^{-2} + 0{\cdot}853\,\alpha_{os} + 0{\cdot}789\,\alpha_{os}^2 - 2{\cdot}023\,\alpha_{os}^3 + 1{\cdot}309\,\alpha_{os}^4. \quad (3)$$

In order to check the results obtained in Fig. 5 the traversing technique and the one-shot method were tried on a series of Lucite mock-ups in the actual geometrical configuration. The Lucite models simulated two preferential phase distribution corresponding to flow patterns encountered in two-phase flow (Fig. 6). In Fig. 7

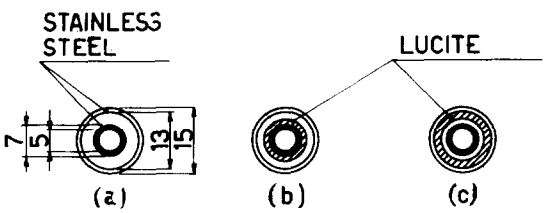

FIG. 6. Lucite mock-ups.
(a) Container.
(b) External voids.
(c) Internal voids.

the actual void values (α_s) are compared with the values measured both by the one-shot (α_{os}) and the traversing technique. From Fig. 7 it is clear that a very good agreement exists between actual and measured void values when

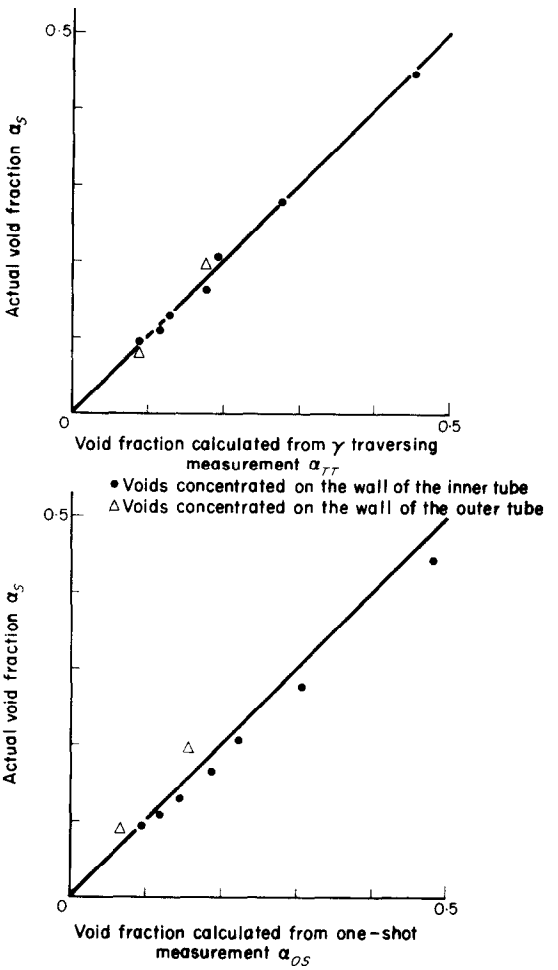

FIG. 7. Lucite mock-up experimental results.

traversing technique is used, for both vapour distributions. Errors occur when one-shot technique is used, which are positive for internal voids and negative for external voids.

2. CONSIDERATIONS ON THE EXPERIMENTS AND RESULTS

For a given test condition (W, T_{in}, Γ) two density measurements were necessary: one under two-phase and the other under liquid flow conditions. The procedure for the two cases

was identical except that no power was supplied to the test section during a water run. As a matter of convenience, considering warm-up time, etc., the water run was usually done first. Each day at the start of the measurements only a run with empty test section was carried out: however, in view of the fact that the source intensity decreases with time, a water run was taken with each set of test conditions. When the system had come into equilibrium under a given test condition, the data constituting a "run" were recorded, i.e. flowmeter reading, test section pressure drop, readings of thermocouples, total count for a given time period, etc.

As above written the first purpose of the experiment was to check the reliability of the γ-absorption method in a small annulus with thick stainless steel walls. The good reliability of the method allowed us to obtain some information in the subcooled and in the bulk boiling range for the annular geometry.

The subcooled forced convection boiling is one of the most important non-thermal equilibrium two-phase flow processes. In such a system heat is being added to a subcooled fluid as it flows past a heated surface and vapour bubbles and liquid below saturation can be found simultaneously at a given cross-section. The boiling flow can be broken down into four regions as suggested by Bowring and Levy [2, 3].

In the first no vapour is present and normal convection cooling prevails; in the second the first vapour bubble appears and more and more bubbles are formed; in the third region the thickness of the superheated liquid layer close to the wall become greater, the bubbles grow to a size large enough to leave the surface and the vapour volumetric fraction starts to rise sharply. In such a region, even though the void fraction is large, non-thermal equilibrium conditions exist, i.e. some of the flowing liquid is still subcooled and the vapour weight fraction is higher than would be calculated from a heat balance. In the fourth region (the bulk boiling one) all the liquid is at saturation temperature and thermal equilibrium conditions have finally been established. The physical boundary between the second and the third region is called the initial point of net vapour generation: the corresponding degree of subcooling θ_d (in the point of rapid rise in subcooled void fraction) greatly affects the following trend of the void fraction, at least in the subcooled region, corresponding to a given heat flux value and mass velocity. The first-order importance for the correct prediction of this point is recognized and illustrated in [4]. It is also pointed out that even the best model for the prediction of the subcooled void fraction in the region of net vapour generation is only as accurate as the method for the prediction of its inception point will allow it to be.

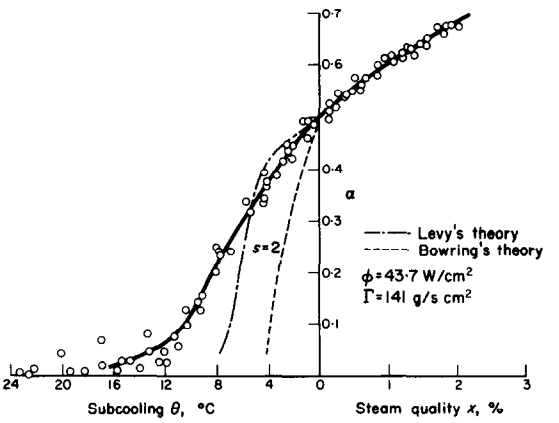

FIG. 8. Void fraction vs. steam quality.

The experiments have been carried out nearly at 1·15 kg/cm^2 pressure, for two values of mass velocity and three different heat fluxes (Figs. 8–12):

Γ = 60·7 g/cm^{2}s, heat flux = 44·6—63·4—88·8 W/cm^2.

Γ = 141·3 g/cm^{2}s, heat flux = 43·7—88·5 W/cm^2.

The following procedure has been applied in data reduction:

(a) Thermal balance of test section by electrical

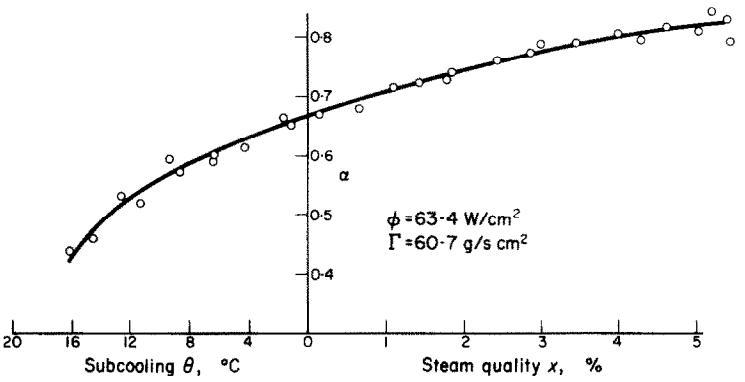

FIG. 9. Void fraction vs. steam quality.

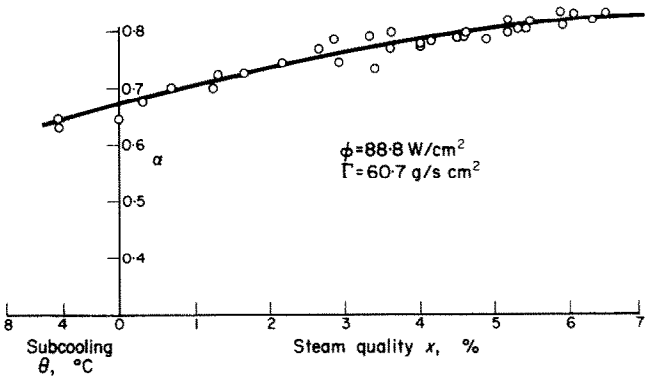

FIG. 10. Void fraction vs. steam quality.

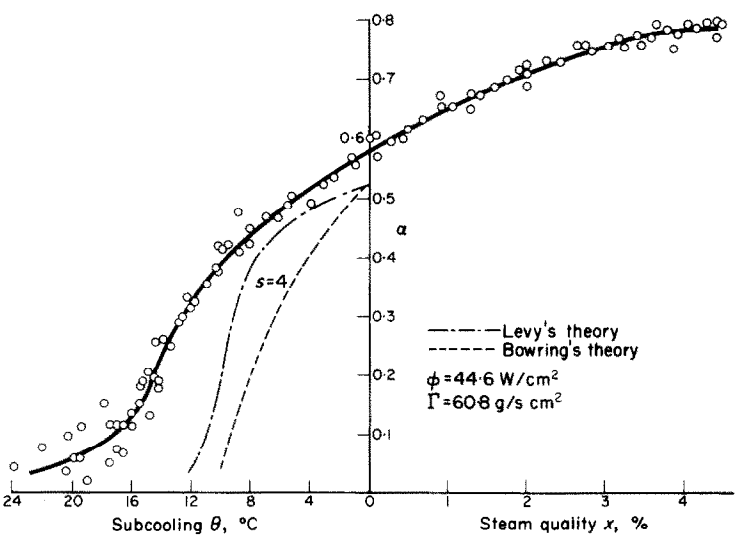

FIG. 11. Void fraction vs. steam quality.

power measurement and by thermodynamic equation; the two procedures have always given results in agreement within 1–3 per cent and this fact proves the reliability of the results.

(b) Evaluation of mixture average local temperature, in thermodynamic equilibrium

(d) Determination of local steam quality by equation (1) $T_{\gamma\,\mathrm{sat.}}$ is the saturation temperature which is calculated taking in account the variation of the local pressure along the test section, as consequence of the hydrostatic height and the frictional pressure drop.

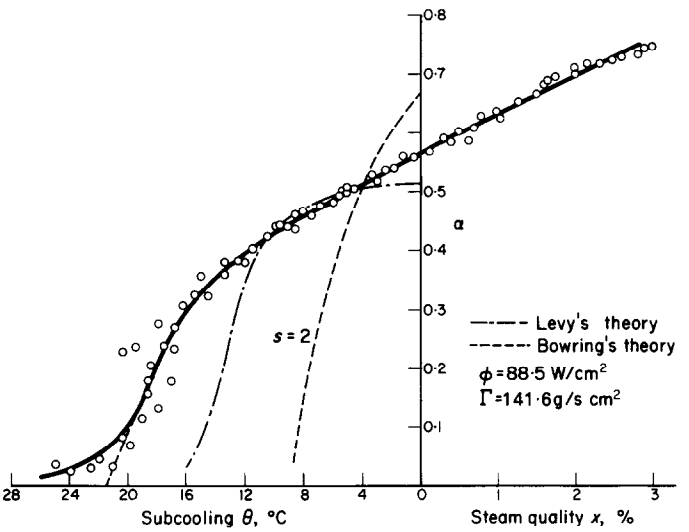

FIG. 12. Void fraction vs. steam quality.

conditions, for the cross section corresponding to the position of the γ-beam axis, from the equations:

$$\left.\begin{aligned} T_{ou} < T_{\mathrm{Sat.}} \qquad & T = T_{in} + (T_{ou} - T_{in})\,\frac{L_\gamma}{L} \\ T_{ou} = T_{\mathrm{sat.}} \qquad & T = T_{in} + \frac{W \cdot L_\gamma}{\Gamma \cdot A_F \cdot c_p \cdot L} \end{aligned}\right\} \quad (4)$$

(c) Determination of local thermodynamic subcooling

$$\left.\begin{aligned} T_{ou} < T_{\mathrm{sat.}} \qquad & \theta = T_{\gamma\,\mathrm{sat.}} - T_\gamma = T_{\gamma\,\mathrm{sat.}} \\ & \quad - T_{in} - (T_{ou} - T_{in})\,L_\gamma / L \\ T_{ou} = T_{\mathrm{sat.}} \qquad & \theta = T_{\gamma\,\mathrm{sat.}} - T_\gamma = T_{\gamma\,\mathrm{sat.}} \\ & \quad - T_{in} - \frac{W \cdot L_\gamma}{\Gamma \cdot A_F \cdot c_p \cdot L} \end{aligned}\right\} \quad (5)$$

(e) Determination of α_{OS} and α_{TT}.

During the measurements there have always been very stable conditions, with small statistical fluctuations of physical parameters, because the flow rate was very constant and the temperature automatic control was very effective with a maximum noise of $\pm 0{\cdot}05$°C for the inlet test section temperature. The results are congruent with low scattering and have been compared with Bowring's [2] and Levy's [3] models in the subcooled region. These models seem to be the most elaborate ones among the several existing theories [5–7]. The theoretical values of void fraction have been calculated only in the high voidage region, because both models are not very significant and accurate in the low voids region. The basic equations of the Bowring

theory at atmospheric pressure are

$$\theta_d = 14{\cdot}1\frac{\phi \cdot \rho_l}{\Gamma} \tag{6}$$

$$\alpha = \alpha_w + \alpha_b \tag{7}$$

where $\alpha_w = \dfrac{P \cdot \delta}{A_F}$ and δ is the less of $\delta = 0{\cdot}066\, R_d$

and $\delta = \dfrac{P_r \cdot K_{th} \cdot \Gamma}{1{\cdot}07 \cdot \rho_l \cdot h^2}$

$$x^* = \frac{c_p}{H_{fg}}\frac{1}{1+\varepsilon'}(\theta_d - \theta) \tag{8}$$

$$\varepsilon' = 1 + 3{\cdot}2\left(\frac{\rho_l}{\rho_{va}}\frac{c_p}{H_{fg}}\right) \tag{9}$$

great uncertainty. From the equation:

$$S = \frac{\rho_l}{\rho_{va}}\left(\frac{1-\alpha}{\alpha}\right)\left(\frac{x}{1-x}\right)$$

we have calculated the slip ratio values in the positive steam quality region: in Fig. 13 these have been plotted for two values of mass velocity and heat flux. As regard to the calculations of the subcooled voids we have chosen $S = 2$–4 corresponding to $\Gamma = 141{\cdot}3$–$60{\cdot}7$ g/scm^2, according to the results reported in [8].

The most important Levy's equations are:

$$Y_B^+ = 0{\cdot}015\sqrt{(\sigma \cdot D_H \cdot \rho_1)}\frac{1}{\mu_l} \tag{11}$$

and corresponding to the values of such a parameter

$$\left.\begin{aligned}
\theta_d &= \frac{\phi}{h} - Q \cdot P_r \cdot Y_B^+ && 0 \leqslant Y_B^+ \leqslant 5\\
\theta_d &= \frac{\phi}{h} - 5Q\left\{P_r + \ln\left[1 + P_r\left(\frac{Y_B^+}{5} - 1\right)\right]\right\} && 5 \leqslant Y_B^+ \leqslant 30\\
\theta_d &= \frac{\phi}{h} - 5Q\left\{P_r + \ln\left[1 + 5P_r\right] + 0{\cdot}5\ln\left(\frac{Y_B^+}{30}\right)\right\} && Y_B^+ \geqslant 30
\end{aligned}\right\} \tag{12}$$

where $Q = \dfrac{\phi}{\rho_l c_p \sqrt{(\tau_w/\rho_l)}}$; $\quad \tau_w = \dfrac{f}{8\rho_l}\Gamma^2$; $\quad f = 5{\cdot}5 \cdot 10^{-3}\left\{1 + \left[2 \cdot 10^{-4}\dfrac{\varepsilon}{D_H} + \dfrac{10^6}{(\Gamma \cdot D_H/\mu_l)}\right]^{\frac{1}{3}}\right\}$.

$$\frac{\alpha_b(1-x^*)}{1-\alpha_b} = \frac{\rho_l}{\rho_{va}} \cdot \frac{c_p}{H_{fg} \cdot S} \cdot \frac{1}{1+\varepsilon'}(\theta_d - \theta). \tag{10}$$

In such a theoretical evaluation of α_b there is the uncertainty in the choice of S value. In fact, at low pressure, S in net boiling conditions is strongly influenced by several factors and may vary in a wide range. The extrapolation of S values, determined in positive low quality region, to subcooled boiling region gives a

The true local vapour weight fraction (or actual mass quality) is expressed by

$$x^* = \frac{c_p}{H_{fg}}\left\{\theta_d \cdot \exp.\left(\frac{\theta}{\theta_d} - 1\right) - \theta\right\}. \tag{13}$$

This equation specifies the value of x^* once the parameters θ and θ_d have been calculated from the method above proposed. Levy obtained the corresponding vapour volumetric fraction by assuming that the relationship between α and

x^* is the same as it would be under thermal equilibrium conditions. Under the several correlations available in the literature Levy uses the following equation proposed by Zuber and Findlay [9]

$$\alpha = \frac{x^*}{\rho_{va}}\left\{C_0\left[\frac{x^*}{\rho_{va}} + \frac{1 - x^*}{\rho_l}\right] + \frac{1 \cdot 18}{\Gamma}\left[\frac{\sigma \cdot g \cdot (\rho_1 - \rho_{va})}{\rho_l^2}\right]^{0 \cdot 25}\right\}^{-1} \quad (14)$$

The value of the distribution parameter C_0 depends on the flow and concentration profiles: we have chosen, for the small annular geometry $C_0 = 1 \cdot 5$.

The values of θ_d, which is the most important parameter in determining the trend of the curve $\alpha - x$ or $\alpha - \theta$ in the subcooled boiling range shows noticeable differences at atmospheric pressure when it is calculated by equation (6) or equation (12). At atmospheric pressure and with the geometrical configuration of the test section shown in Fig. 1 it results, according to the equation (11), $Y_B^+ > 30$: therefore

$$\text{Bowring's model } \theta_d = 14 \cdot 1 \frac{\phi \cdot \rho_l}{\Gamma} \quad (15)$$

$$\text{Levy's model } \theta_d = \phi \cdot \Gamma^{-0 \cdot 8} \cdot [f_1(D_H, \mu_l K_{th}, c_p) + f_2(\varepsilon/D_H, \Gamma, D_H, \mu_l, K_{th}) + f_3(\varepsilon/D_H, \Gamma, D_H, \mu_l, c_p, \sigma, \rho_l)]. \quad (16)$$

Both models agree what concerns the dependence of θ_d from the heat flux ϕ, but according to the Bowring's theory θ_d depends only on mass velocity, heat flux and density. On the contrary Levy's model introduces the influence on θ_d of mass velocity, heat flux, physical constants and geometry (through the hydraulic diameter D_H).

In Figs. 8–12 we have reported for comparison with our experimental results the functions $\alpha - \theta$ in the subcooled region calculated according to the equations (6) and (12), (10) and (14). It appears clear that the phenomenon of the net inception boiling in the subcooled region is better depicted from the much more complete expression of θ_d contained in (16) than from the (15). The poor agreement between the theoretical Bowring's predictions and the experimental values of θ_d is not surprising, since an annular cross-section with only the inside perimeter being heated falls outside of the geometries covered in deriving the criterion. Nevertheless also the values of θ_d computed according to the (16) are always smaller than the experimental ones. We have:

$\phi = 43 \cdot 7\ \text{W/cm}^2$; $\Gamma = 141\ \text{g/scm}^2$;
$\theta_{BO} = 4 \cdot 2°\text{C}$; $\theta_{LE} = 7 \cdot 7°\text{C}$; $\theta_{\text{exp.}} = 12 \cdot 7°\text{C}$

$\phi = 88 \cdot 5\ \text{W/cm}^2$; $\Gamma = 141 \cdot 6\ \text{g/scm}^2$;
$\theta_{BO} = 8 \cdot 7°\text{C}$; $\theta_{LE} = 15 \cdot 8°\text{C}$; $\theta_{\text{exp}} = 21 \cdot 5°\text{C}$

$\phi = 44 \cdot 6\ \text{W/cm}^2$; $\Gamma = 60 \cdot 8\ \text{g/scm}^2$;
$\theta_{BO} = 10°\text{C}$; $\theta_{LE} = 12°\text{C}$; $\theta_{\text{exp}} = 17 \cdot 7°\text{C}$.

Comparison of curves of void fraction vs. quality for conditions differing only in the value of flow rate or only in the value of heat flux leads to the results schematically shown in Figs. 14 and 15. These repeat once again the very great importance of the detachment subcooling θ_d, whose dependence from heat flux and mass velocity determine the trend of the

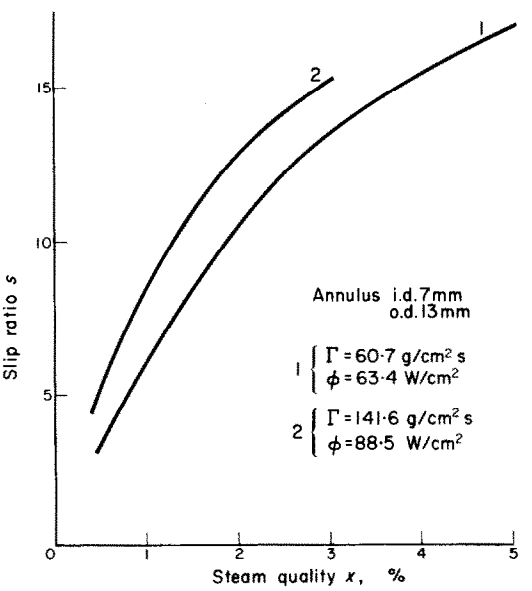

FIG. 13. Slip ratio vs. steam quality.

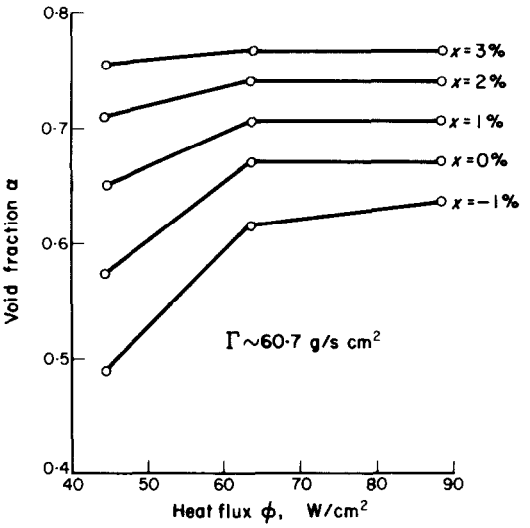

FIG. 14. Void fraction vs. heat flux.

functions α–Γ and α–ϕ. Therefore in the bulk boiling region, for steam qualities higher than 3 per cent, where the effects of θ_d become smaller and smaller, the void fraction, within the limits of experimental errors, become independent from heat flux and mass velocity. Although the range of heat fluxes and mass velocities is very limited, giving a much smaller picture of this effect than would be desired, taking into account the particular influence of ϕ and Γ on θ_d, i.e. their influence in the subcooled region on the void fraction, the trends reported in Figs. 14 and 15 seem reasonable.

ACKNOWLEDGEMENTS

The authors are especially indebted to Mr. Robert Festoso and to Mr. Gianfranco Canti for the assistance in carrying out the experimental measurements.

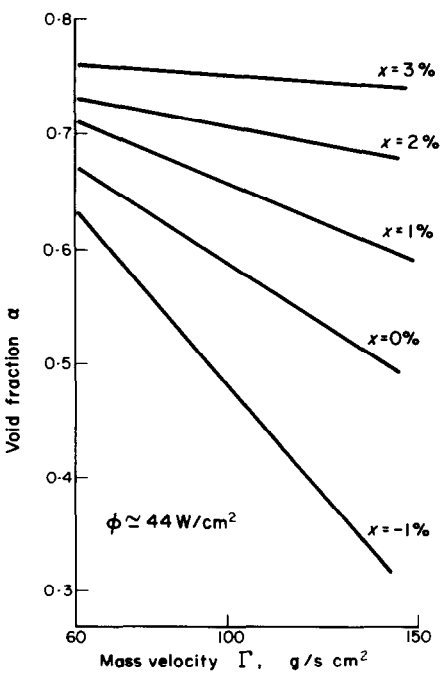

FIG. 15. Void fraction vs. mass velocity.

REFERENCES

1. L. CIMORELLI and R. EVANGELISTI, The application of the capacitance method for void fraction measurement in bulk boiling conditions, *Int. J. Heat Mass Transfer* **10**, 277–288 (1967).
2. R. W. BOWRING, Physical model, based on bubble detachment and calculation of steam voidage in the subcooled region of a heated channel, OECD Halden Reactor Project, **10** (1962).
3. S. LEVY: Forced convection subcooled boiling: prediction of vapor volumetric fraction, *Int. J. Heat Mass Transfer*, **10**, 951–965 (1967).
4. F. W. STAUB: The void fraction in subcooled boiling. Prediction of the initial point of net vapor generation, 9th National Heat Transfer Conference, Seattle, Washington, August 1967, Paper No. 67-HT-36.
5. P. GRIFFITH: The prediction of low quality boiling void, ASME Paper No. 63-HT-20 (1963).
6. N. ZUBER, F. W. STAUB and G. BIJWAARD: Vapor void fractions in subcooled boiling and in saturated boiling systems, Third International Heat Transfer Conference, Chicago, Illinois, August, 1966.
7. S. ZIA ROUHANI, Calculation of steam volume fraction in subcooled boiling, 9th National Heat Transfer Conference, Seattle, Washington, August 1967, Paper No. 67-HT-31.
8. L. CIMORELLI and A. PREMOLI, Measurement of void fraction with impedance gauge technique, *Energia Nucl.* **13**, 12–23 (1966).
9. N. ZUBER and J. FINDLAY, Average volumetric concentration in two-phase flow systems, *Am. Soc. Mech. Engrs J. Heat Mass Transfer* (C) **87**, 453–468 (1965).

Résumé—L'application de la méthode d'absorption de rayons γ de la fraction volumique de vapeur pendant l'ébullition par convection dans un petit canal annulaire est discutée.

Les résultats expérimentaux sont présentés et comparés avec les modèles théoriques existants dans la région sous-rerroidie.

Zusammenfassung—Die Anwendung der γ-Absorptionsmethode zur Messung des Dampfvolumenanteils beim Konvektionssieden in einem kleinen ringförmigen Kanal wird diskutiert.

Die experimentellen Ergebnisse werden angegeben und mit bestehenden theoretischen Modellen im unterkühlten Gebiet verglichen.

Аннотация—Рассматривается применение абсорбционного метода для измерения объемной концентрации пара в процессе конвективного кипения в узком кольцевом канале. Экспериментальные результаты сравниваются с существующими теоретическими методами в недогретой области.